Available online at www.sciencedirect.com
ScienceDirect
Journal of Photochemistry and Photobiology A: Chemistry 197 (2008) 394–401
Journal of Photochemistry and Photobiology A:Chemistry
www.elsevier.com/locate/jphotochem

Photodynamic action of bis(tertiary arsine (diars)) metal(III) complexes *trans*-$[M(diars)_2X_2]^+$ (X = Cl, Br, I); M = Co^{3+}, Cr^{3+}, Rh^{3+}: Optical and EPR spin-trapping studies

A. Suganthi [a,*], M. Rajarajan [b], R. Murugesan [c]

[a] *Post Graduate and Research Department of Chemistry, Thiagarajar College (Autonomous), Teppakulam, Madurai 625009, Tamil Nadu, India*
[b] *Department of Chemistry, C.P.A. College, Bodinayakanur 625513, India*
[c] *School of Chemistry, Madurai Kamaraj University, Madurai 625021, India*

Received 6 September 2007; received in revised form 17 January 2008; accepted 7 February 2008
Available online 15 February 2008

Abstract

Photodynamic properties of series of metal complexes having the general formula $[M(diars)_2X_2]ClO_4$ or BF_4 where M = Co^{3+}, Cr^{3+}, Rh^{3+}; X = Cl, Br, I, diars = *o*-phenylene bis(dimethylarsine) are studied. Photogeneration of singlet oxygen is monitored by both optical and EPR methods. In comparison with rose bengal ($\phi(^1O_2)$ for RB = 0.76), singlet oxygen generating efficiencies of these complexes are determined. Rate of *N*,*N*-dimethyl-4-nitrosoaniline (RNO) bleaching is found to be retarded by specific $^1O_2$ quencher NaN_3, confirming the involvement of $^1O_2$ as an active intermediate. Photolysis of these complexes in the presence of spin trap 5,5-dimethyl-1-pyrroline-*N*-oxide (DMPO) generates 12-line EPR spectra, characteristic of $O_2^{\bullet-}$ adduct. Photogeneration of $O_2^{\bullet-}$ is also monitored by optical spectroscopy using superoxide dismutase (SOD) inhibitable cytochrome *c* reduction assay. The results indicate that the $[Co(diars)_2Br_2]ClO_4$ complex possesses high ability to generate reactive oxygen species (ROS). Both Type I and II paths are involved in the photosensitisation of the metal complexes. The antimicrobial activity of the complexes against selected bacteria is estimated. The relationship between the enzymatic production of ROS and antimicrobial activity of the complexes is examined and a good correlation between two factors is found. The $[CoBr_2(diars)_2]ClO_4$ complex investigated in this study effect photo cleavage of the plasmid DNA (pUC18).

Keywords: Metal diars complexes; ROS generation; Spin trapping; DNA strand break; EPR

1. Introduction

o-Phenylene bis(dimethylarsine), known as diars, acts as a versatile ligand and is capable of stabilizing a range of oxidation states of many transition elements [1]. Diars complexes have attracted interest in the field of radiopharmaceuticals because of the observation of selective uptake of $[Tc(diars)_2Cl_2]Cl$ in the brain tissue of test animals [2,3]. Tc that incorporate tertiary arsine ligands are developed as myocardial imaging agents [4]. The analogous ^{186}Re complexes has also been investigated with regard to their potential use in nuclear medicine [5]. Numerous metal complexes have been screened for their wide-ranging antivirus, antimicrobial and antiinflammatory activities [6–9]. It is known that metal complexes induce toxic effects through generation of reactive oxygen species (ROS) [10,11]. ROS produced may be involved in cellular damage [12,13]. ROS such as hydroxylradicals, superoxide anions, hydrogen peroxide and singlet oxygen leads to lipid peroxidation. ROS plays a vital role in the oxidative damage of DNA in biological process including mutagenesis, carcinogenesis, aging, radiation effects and in the action of several anticancer drugs such as adriamycin and bleomycin [14,15]. In general, studies on photoexcitation of metal complexes in relation to generation of ROS are limited. This consideration prompted us to investigate photodynamic action of $[M(diars)_2X_2]^+$ complexes, where X = Cl, Br, I; M = Cr, Co, Rh. The present study reports the photogeneration of $^1O_2$ and superoxide anion from diars complexes. Optical and EPR spin-trapping techniques are used to investigate the

* Corresponding author. Tel.: +91 452 2311875; fax: +91 452 2312375.
E-mail address: suganthitc@yahoo.com (A. Suganthi).

1010-6030/$ – see front matter © 2008 Elsevier B.V. All rights reserved.
doi:10.1016/j.jphotochem.2008.02.006

transient products ($^1O_2$, $O_2^{\bullet -}$, $^\bullet OH$). The effect of electron donors such as ethylenediaminetetraacetic acid (EDTA) and reduced nicotinamide adenine dinucleotide (NADH) on the efficiency of photogeneration of superoxide anion is also presented here. We also report the antimicrobial activity and photo-induced plasmid DNA strand break by these metal complexes.

2. Materials and methods

2.1. Chemicals

Metal complexes were received as gift from Prof. M.A. Bennet and recrystallized from ethanol [16]. The general structure of metal complexes is shown in Fig. 1.

Superoxide dismutase (SOD), catalase and cytochrome *c* were purchased from Sigma Chemicals Co., while reduced NADH was obtained from Boehringer Mannheim. Dimethyl sulphoxide (HPLC grade) was procured from Qualigens Fine Chemicals, India. *N*,*N*-Dimethyl-4-nitrosoaniline (RNO), 1,4-diazabicyclo-[2,2,2]-octane (DABCO), diethyltriaminopentaacetic acid (DETAPAC) and rose bengal (RB) were obtained from Aldrich. The spin trap 5,5-dimethyl-1-pyrroline-*N*-oxide (DMPO) was obtained from Aldrich and was purified by activated charcoal [17]. 2,2,6,6-Tetramethyl piperidinol (TEMPL) was obtained from Merck, India. Imidazole, EDTA and sodium azide were purchased from S.D. Fine Chemicals, India. Imidazole was used after repeated crystallization from double-distilled water. All other compounds were used as received.

2.2. Light source

Light source used for irradiation was a 150-W xenon lamp. A filter combination of 10-cm potassium iodide solution (1 g in 100 ml) and 1-cm pyridine was used to cut-off below 300 nm and to achieve a spectral window of 300–700 nm. The irradiation was generally carried out in an open cuvette, in equilibrium with the atmosphere. The reaction mixture in a quartz cuvette, placed at a distance of 12 cm from the light source was continuously stirred during irradiation.

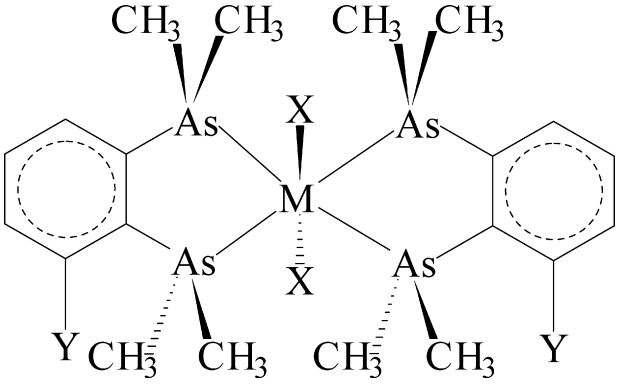

Fig. 1. Structure of *o*-phenylene bis(dimethyl arsine) metal complexes. Complex **1**: M = Cr, X = Cl; complex **2**: M = Co, X = Cl, Y = CH_3; complex **3**: M = Co, X = Br; complex **4**: M = Co, X = I; complex **5**: M = Rh, X = Cl.

2.3. Optical assay

2.3.1. Detection of singlet oxygen

The singlet oxygen generating efficiencies of the metal complexes were measured by RNO bleaching assay. Photoexcitation of the sensitiser generates $^1O_2$ which bleaches RNO and the bleaching can be monitored spectrophotometrically at 440 nm [18]. The sensitiser was exposed to light in the presence of imidazole (10 mM) and RNO (50 mM) in phosphate buffer (pH 7.4). The intermediacy to $^1O_2$ in bleaching RNO is further confirmed by carrying out the reaction in the presence of scavengers specific to $^1O_2$ and following the inhibition of RNO bleaching. Shimadzu UV–vis Spectrometer (UV-160) as well as Specord S100 UV–vis Spectrometer Analytik Jena AG, Jena, Germany were used for optical measurements. The interference of $O_2^{\bullet -}$ and H_2O_2 on RNO bleaching was removed by the addition of SOD and catalase, respectively.

The rate of disappearance of quencher [*A*] obeys the following equation [19]:

$$\frac{-\mathrm{d}[A]}{\mathrm{d}t} = \{I_{ab}\phi(^1O_2)\}\frac{K_r[A]}{K_d}$$

where K_r is the rate constant for chemical quenching, K_d is the rate constant for deactivation of $^1O_2$ by the solvent, and I_{ab} is the intensity of light absorbed by the sensitiser. The slope of the first-order plot is $I_{ab}\ \phi(^1O_2)\ (K_r/K_d)$. The slope was calculated by curve fitting the experimental data. The quantum yield for the complexes studied was determined based on the relative rates of RNO bleaching, under identical conditions, with reference to singlet oxygen generator RB. The relative rate of slopes were corrected for molar absorption and photon energy [20]. $^1O_2$ quantum yield for RB is taken as 0.76 [21]. The details of the calculation is presented elsewhere [22].

2.3.2. Superoxide detection—SOD inhibitable cytochrome *c* reduction assay

The generation of superoxide was detected by the reduction of Fe(III)–cyt. *c* with $O_2^{\bullet -}$. Solution of metal complexes (100 μm) were photolysed in the presence of ferricytochrome *c* (50 μm) in 50-mM phosphate buffer solution (pH 7.4). The increase in absorbance was monitored spectrophotometrically at 550 nm, using $\Delta\varepsilon_{550} = 20{,}000\ M^{-1}\,cm^{-1}$ for the reduced–oxidised cytochrome *c* [23,24]. To study enzymatic production of superoxide, similar experiments were carried out with cytochrome *c* reductase in the dark. The reduction of ferricytochrome *c* (40 μM) in the presence of NADH (3 mM), cytochrome *c* reductase (30 mg/ml), DETAPAC (100 mM) and metal complexes (100 μM) in 50-mM phosphate buffer solution (pH 7.4) was monitored at 550 nm by an increase of the absorbance with time [25].

2.4. EPR measurements

A JEOL JES-TE100 X-band Spectrometer was used for EPR measurements. The following parameters were set for the measurements: microwave power, 10 mW; modulation amplitude, 0.01 mT; modulation frequency, 100 kHz.

2.4.1. Detection of singlet oxygen

The detection of $^1O_2$ by EPR was also used as an alternative method to determine the photogeneration of $^1O_2$. The EPR–TEMPL experiment was carried out for RB, and the metal complexes under identical conditions. The reaction mixture (1 ml) containing 0.02 M TEMPL and 0.1 mM complexes in DMSO was irradiated and the increase in EPR signal intensity was followed as a function of time. TEMPOL, a stable nitroxide free radical, formed as a result of oxidation of TEMPL by $^1O_2$ shows a three-line EPR spectrum. The formation of EPR signal intensity of TEMPOL was not observed in dark. Samples were injected into gas-permeable Teflon capillary tube (0.8-mm inside diameter, 0.5-mm wall thickness) which was folded and inserted into a narrow quartz tube and placed in the EPR cavity for measurements [26,27]. The increase in EPR signal intensity of the TEMPOL (2,2,6,6-tetramethyl-4-piperidinol-*N*-oxyl) radical produced with irradiation time was followed.

2.4.2. Detection of superoxide anion

EPR spin-trapping experiments were also used to detect the generation of $O_2^{\bullet -}$ on photoirradiation of metal complexes. Solutions of metal complexes (100 μM) were irradiated in the presence of 40 mM DMPO in DMSO. Experiments were repeated to monitor the signal intensity at different intervals of irradiation time. The transient radical species were trapped by DMPO to form DMPO adducts. The spectral identification of the spin adducts was confirmed by simulating the spectra with known hyperfine coupling constants (hfcc) and comparing them with the experimentally observed one. A BASIC program was used to simulate the EPR spectra.

2.5. Biological activity: antibacterial tests

Fresh solutions of metal complexes in DMSO (0.15%) were prepared and used for biological assays. Well diffusion assay described by Schillinger and Lucke [28] was used for the testing of antagonistic activities of selected complexes against common human pathogens of *Staphylococus aureus* (Gram-positive bacteria) and *Escherichia coli* (Gram-negative bacteria). Four wells, each 7 mm in diameter were made in the agar using cork borer and 10–50 ml of samples of complexes were transferred to each well. The plates were incubated for 24 h at 37 °C and examined for clear inhibition zone around the well. The assay was carried out in duplicate for both the test organisms.

2.6. Cyclic voltammetry

Cyclic voltammetry was carried out with the electrochemical analyser BAS 50A. For electrochemical experiment, a thick electrode cell configuration was utilised. This assembly consisted of glassy-carbon working electrode, platinum wire auxiliary electrode and Ag/AgCl reference electrode. Glassy-carbon electrode was resurfaced with alumina. Solutions of the metal complexes (0.001 M) were prepared in HPLC grade DMSO containing 0.05 M tetrabutyl ammonium perchlorate (TBAP) as supporting electrolyte. Each solution was deoxygenated for 5 min with purified nitrogen prior to measurements and the cyclic voltammograms were recorded under nitrogen atmosphere. The redox potentials given are against Ag/AgCl, unless otherwise mentioned.

2.7. Photo cleavage of DNA by metal complexes

Covalently closed circular (ccc) pUC18 plasmid DNA was prepared and purified by the method of Maniatis et al. [29]. The air-saturated solution containing DNA (3 μg) and metal complexes (1 mM) in phosphate buffer (pH 7.4) were irradiated in a gas-permeable Teflon tube. After the irradiation was over, 20-μl aliquot of the mixture was loaded into agarose gels (0.7%) in Tris–acetate–EDTA buffer, containing 0.05 μg/ml ethidium bromide. The electrophoresis was carried out for 1 h at 50 V. After electrophoresis, the gels were illuminated with UV light and photographed.

3. Results and discussion

3.1. Biological activities

The *in vitro* antimicrobial activity of the metal complexes **1** and **3** was evaluated against representative Gram-positive, and Gram-negative bacteria. The MIC is reported in Table 1. Complexes **1** and **3** were active against *Staphylococcus aureus* (Gram-positive bacteria) with MIC in the range of 10–14 μg/ml. Antibacterial activity against *E. coli* (Gram-negative bacteria) of same complexes **1** and **3** showed MIC values ranges from 18 to 22 μg/ml.

3.2. Singlet oxygen generation

Generation of $^1O_2$ was measured by RNO bleaching assay. The loss of RNO absorbance at 440 nm as a function of irradiation time for metal complexes (**1**–**5**) is shown in Fig. 2. Singlet oxygen generated by photoexcitation of metal complexes reacts with imidazole to form transannular peroxide which bleaches the RNO. The bleaching of RNO is caused by the transannular peroxide intermediate formed as a result of reaction between photogenerated $^1O_2$ and imidazole. The bleaching rate is used for calculating $^1O_2$ yield. The ratio of slopes of RB to each sensitiser was corrected for molar absorption and photon energy to obtain the singlet oxygen generating efficiencies of metal complexes. SOD (50 μg/ml) and catalase (40 μg/ml) which remove $O_2^{\bullet -}$ and H_2O_2 from the reaction mixture, respectively were added to permit the detection and quantification of $O_2^{\bullet -}$ pro-

Table 1
Antimicrobial activity of complexes[a]

Species	Complex	
	1	**3**
Staphylococus aureus	14	10
E. coli	22	18

All experiments were carried out in duplicate and average results are given.
[a] Values represent minimum inhibitory concentration (MIC, μg/ml).

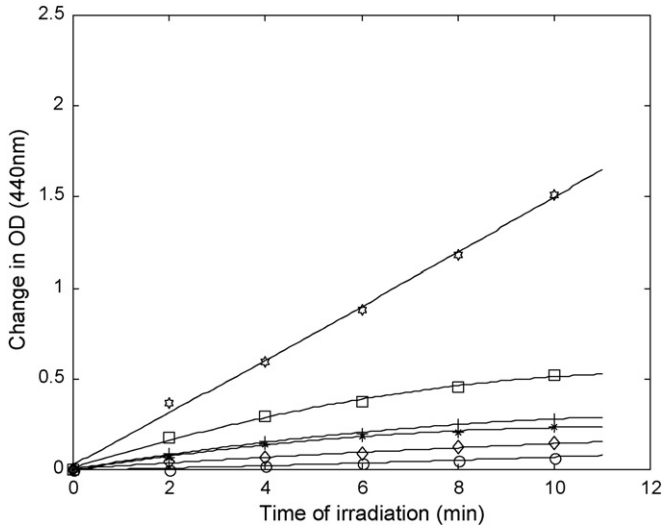

Fig. 2. Photosensitised RNO bleaching measured at 440 nm in the presence of imidazole (10 mm) in 50-mM phosphate buffer (pH 7.4) with RB (☆), complex **3** (□), **4** (+), **2** (*), **5** (◊), **1** (◯) as a function of illumination of time in minutes. The slope was calculated by curve fitting the experimental data.

duction, without interference from OH radical. Complexes **3** and **4** showed greater efficiency of singlet oxygen production.

To confirm the production of $^1O_2$, experiments were carried out in the presence of specific $^1O_2$ quencher sodium azide. The concentration of sodium azide used was 0.1 mM. At this concentration, it was found that the RNO bleaching was inhibited by 50%. This is indicated in Fig. 3. These results confirm the generation of $^1O_2$ during photodynamic process [30]. The quantum yields thus evaluated are 0.02, 0.24, 0.54, 0.44 and 0.13 for the metal complexes **1**–**5**, respectively.

The higher quantum yield for the complexes **3** and **4** may be attributed to the long-triplet state lifetime of these complexes [31]. It is interesting to note that the quantum yield of singlet oxygen formation increases as the number of halogen atom increases

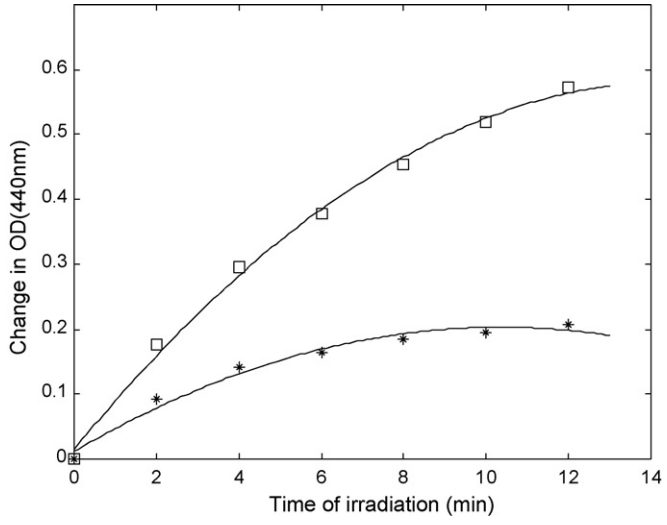

Fig. 3. Photosensitised RNO bleaching by complex 3 in the absence (□) and presence (*) of 0.01 M NaN_3.

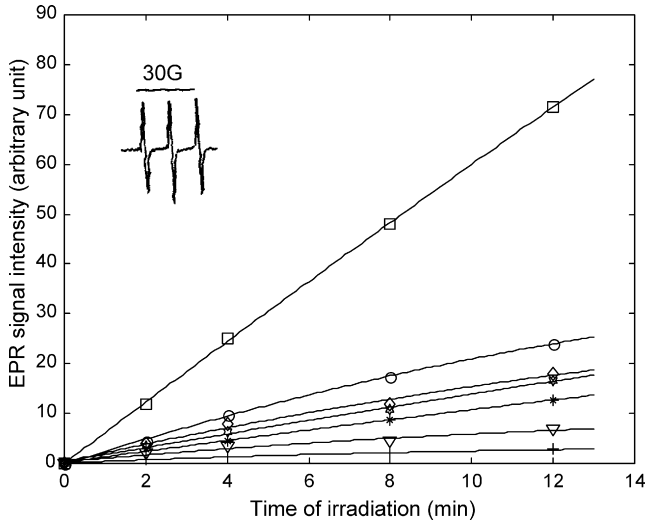

Fig. 4. The formation of TEMPOL during the photoirradiation of RB (□), complex **3** (◯), **4** (◊), **5** (☆), **2** (*), **1** (▽) in the presence of TEMPL (20 mM) at 300 K in DMSO. Inhibitory effects of 2-mM azide (+) on the intensity of TEMPOL radical during photoirradiation of complex **3**. The inset shows EPR spectrum of TEMPOL generated during the photoirradiation of DMSO solution of complex **3** (0.1 mM) in the presence of TEMPL. Spectrometer settings—microwave power: 2 mW; modulation amplitude: 1 G; time constant: 0.1 s; scan rate: 4 min.

in the photosensitisers. This is also in accordance with classical spin–orbit coupling theory [32]. According to this theory, incorporation of a halogen atom is accompanied by a significant decrease in fluorescence quantum yield and lifetime. There is concomitant increase in the quantum yield for formation of the triplet state by promoting intersystem crossing. As expected, the magnitude of these effects increases according to Cl < Br < I and increases proportionately with increasing number of halogen substituents [33]. It is noteworthy that several types of d^6 metal complexes Co(III), Rh(III) induce DNA strand scission by the generation of singlet oxygen. Prevalence of photo substitution over photoredox processes accounts for the lower quantum yield of singlet oxygen for the chromium complex [34].

The generation of $^1O_2$ in photodynamic process was further confirmed by EPR method. Irradiation of oxygen-saturated solution containing the metal complexes (100 μM) and TEMPL (10 mM) gave a typical three-line EPR spectrum of nitroxide at room temperature. The formation of TEMPOL from TEMPL is due to the oxidation by $^1O_2$ as shown in the following equation:

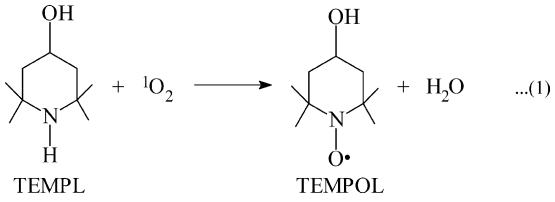

(1)

The hfcc (A_N = 15.7 G) was found to be identical with the literature ascribed to that of TEMPOL [35]. The intensity of EPR signal was found to increase with increase of irradiation time as shown in Fig. 4. Under the same condition RB also showed the formation of TEMPOL. The state of formation of TEMPOL by

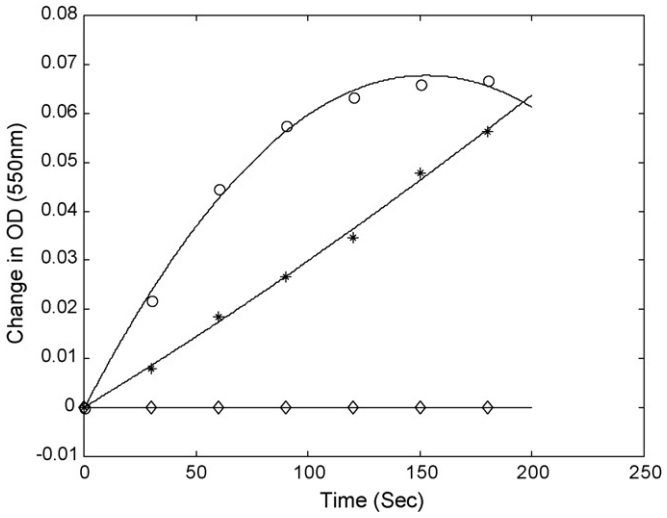

Fig. 5. Enzymatic reduction of cytochrome *c* on the time course in the presence of metal complexes (100 μM) in 50-mM phosphate buffer (pH 7.4) and in the presence of NADH (3 mM), DETAPAC (100 mM) and cytochrome *c* reductase (30 mg/ml). Control: cyt. *c* + NADH + cyt. *c* reductase (◊); control + complex **3** (◯); control + complex **1** (*).

the metal complexes are parallel to their $^1O_2$ generating quantum yields estimated by RNO bleaching method. The relative $^1O_2$ generating ratio of RB and metal complexes (**1**–**5**) were determined to be: 1:0.11:0.18:0.42:0.29:0.22, respectively. Control experiments indicated that, sensitiser, oxygen and light were all essential for the production of TEMPOL, indicating that the formation of the nitroxide radical is a photodynamic process. The addition of sodium azide, a typical $^1O_2$ quencher, inhibited the EPR signal significantly.

3.3. Enzymatic generation of superoxide anion

Fig. 5 shows the reduction of cytochrome *c* as a function of time when air-saturated 50-mM phosphate buffer solution

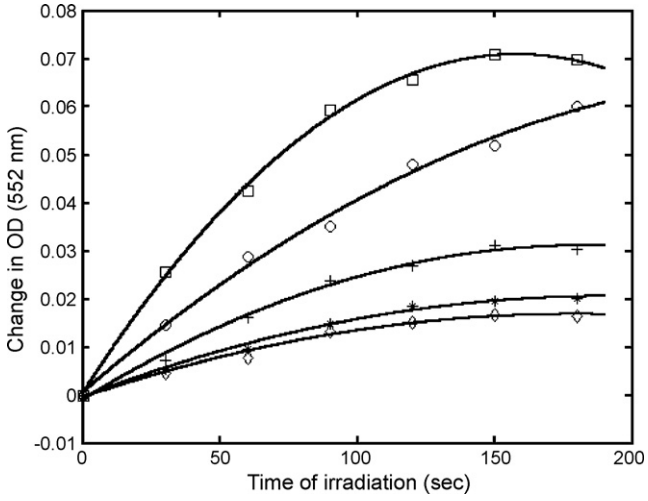

Fig. 6. Photosensitised superoxide generation measured as the rate of cytochrome *c* reduction in 50-mM phosphate buffer, pH 7.4 by complex **3** (□), **4** (◯), **1** (+), **2** (*), **5** (◊), as a function of irradiation time.

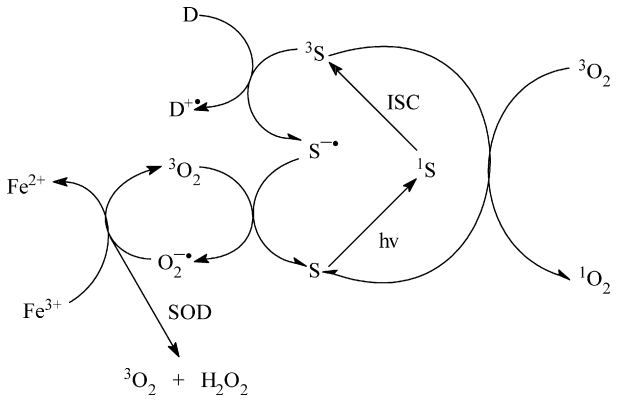

Scheme 1.

containing the metal complexes **1** and **3** (100 μM) was incubated with NADH (3 mM), cytochrome *c* reductase (30 mg/ml) and DETAPAC (100 mM). The reduction efficiency rate of the complexes **1** and **3** are calculated to be 0.13 and 0.24 μM/s, respectively. Addition of SOD inhibited the cytochrome *c* reduction, indicating that superoxide anion is involved in the reduction of cytochrome *c*.

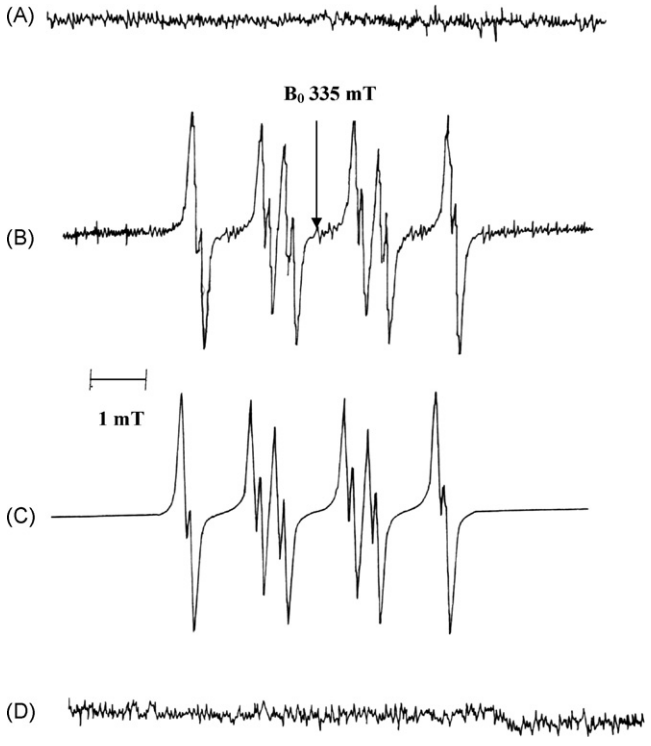

Fig. 7. EPR spectrum obtained by photolysis of complex 3 (100 μM) in air-saturated DMSO solution containing DMPO (50 mM) (A) In the dark; (B) after 4 min irradiation; (C) computer simulated spectrum obtained by the combination of two spin adducts. The spectrum contains two spin adducts: DMPO–$O_2^{\bullet-}$ (A_N = 1.448 mT, A_H^β = 1.08 mT and A_H^γ = 0.10 mT) and DMPO–OH (A_N = 1.37 mT and A_H^β = 1.28 mT) in the ratio 90:10. (D) After 4 min irradiation in the presence of SOD (40 μg/ml). Spectrometer settings—microwave power: 10 mW; modulation amplitude: 0.1 mT; gain level: 6.3×10^3; time constant: 0.1 s; scan rate: 4 min, frequency: 9.39 GHz; g_{iso} = 2.0033.

3.4. Superoxide anion generation

3.4.1. SOD inhibitable cytochrome c reduction assay

Metal complexes on photoillumination in aerobic solution generate superoxide that could be studied by using ferricytochrome *c* reduction assay according to the following equation:

$$\text{Fe(III)–cyt.c} + O_2^{\bullet -} \rightarrow \text{Fe(II)–cyt.c} + O_2 \quad (2)$$

Fig. 6 shows the reduction of cytochrome *c* as a function of irradiation time when air-saturated solutions of the metal complexes were photolysed in the presence of 50 μM cytochrome *c* in phosphate buffer (50 mM and pH 7.4). The rate of superoxide generation was arrived to be 0.18, 0.11, 0.49, 0.29 and 0.075 for the complexes **1**–**5**, respectively. Addition of SOD was found to inhibit the cytochrome *c* reduction. In the presence of electron donor EDTA, the rate of cytochrome *c* reduction was enhanced. Enhancement of generation of superoxide by the sensitisers in the presence of electron donor is indicative of formation of an anionic intermediate ($S^{\bullet -}$) due to the interaction of electron donor with the triplet state of the sensitiser [35] as shown in Scheme 1.

3.5. Spin-trapping assay

The photogenerated $O_2^{\bullet -}$ from metal complexes was studied by EPR spin-trapping experiment using DMPO as the spin trap. Lifetime of the spin adduct of DMPO–$O_2^{\bullet -}$ is short in protic solvent and the superoxide adduct decomposes to DMPO–$^{\bullet}$OH. Hence EPR spin-trapping studies were carried out in DMSO in which the DMPO–$O_2^{\bullet -}$ adduct has longer lifetime [36,37]. Fig. 7 shows the EPR spectrum of complex **3**. No EPR signal was observed either in dark or when DMPO alone was irradiated in DMSO (Fig. 7A). Fig. 7B shows the multiline EPR spectrum obtained when metal complex **3** was photolysed in the presence of DMPO (100 mM) in an air-saturated DMSO solution.

The spectrum can readily be analysed in terms of a mixture of two types of DMPO adducts. Adduct I was assigned to DMPO–$O_2^{\bullet -}$, based on its hfcc $A_N = 1.448$ mT, $A_H^{\beta} = 1.08$ mT and $A_H^{\gamma} = 0.10$ mT. Adduct II was identified as DMPO–OH, with hfcc $A_N = 1.37$ mT and $A_H^{\beta} = 1.280$ mT. The EPR spectra of these two adduct were computer simulated separately using the above hfcc values. When these two spectra were combined in the ratio of 90:10 for $O_2^{\bullet -}$ and $^{\bullet}$OH, respectively, the computer simulated spectra (Fig. 7C) matched well with the experimentally observed one. Addition of SOD (40 μg/ml)

Fig. 8. EPR spectrum generated by irradiation of complex **4** (100 μm) and DMPO (100 μm) in air-saturated DMSO solution. (A) in the dark; (B) after 4 min irradiation; (C) the computer simulated EPR spectrum of DMP–$O_2^{\bullet -}$ adduct using hfcc values $A_N = 1.45$ mT, $A_H^{\beta} = 1.32$ mT and $A_H^{\gamma} = 0.85$ mT and line width used is 0.76 mT; (D) after 4 min irradiation in the presence of SOD. Spectrometer settings—microwave power: 10 mW; modulation amplitude: 0.1 mT; gain level: 6.3×10^3; time constant: 0.1 s; scan rate: 4 min, frequency: 9.40 GHz; g_{iso}: 2.0036.

prior to illumination inhibited the generation of spin adducts, DMPO–$O_2^{\bullet-}$ confirming the photoproduction of $O_2^{\bullet-}$.

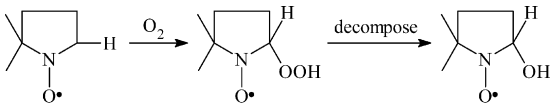

DMPO DMPO - OOH DMPO - OH

Hydroxyl radical may be generated either from the decomposition of DMPO–OOH adduct or may directly be produced from the photoirradiation of the substrates. After addition of excess ethanol, DMPO–OH signal was not abolished, indicating that hydroxyl radical is not generated directly [38]. Hence the DMPO–OH signal was observed due to the decomposition of DMPO–OOH adduct only. All other complexes **1**, **2**, **4**, **5** also gave the DMPO–$O_2^{\bullet-}$ adduct when they were photolysed in the presence of DMPO in air-saturated DMSO solution.

Fig. 8 shows the EPR spectrum of complex **4**. No EPR signal was observed in dark as well when DMPO alone was irradiated in DMSO (Fig. 8A). Irradiation of complex **4** (100 μM) and DMPO (100 μM) in aerated DMSO solution generates a 12-line EPR spectrum characteristic of DMPO–$O_2^{\bullet-}$ adduct (Fig. 8B). The identity of this adduct was further confirmed by using the computer simulated spectrum (Fig. 8C). The hyperfine coupling constants of the spin adduct was analysed as primary nitrogen triplet $A_N = 1.45$ mT split by a proton ($A_H^{\beta} = 1.32$ mT) which in turn further split by a secondary proton (0.085 mT). Addition of SOD prevented the formation of spin adducts as shown in Fig. 8D.

3.6. Redox potentials

Electrochemical studies were carried out to determine the reduction potentials of the complexes. Cyclic voltammogram of the complexes were measured in the range of +1 to −1 V. The electrochemical data for the metal complexes are given in Table 2. The metal diarsine complexes undergo quasi-reversible one electron redox process as revealed by ΔE_p values. Dependence of the rate of formation of superoxide anion on the redox potential is noticed. Complex **3** has a less negative half wave potential ($E_{1/2} = -0.208$ V) than all other complexes and hence it may favour the enzymatic reduction by cytochrome *c* reductase [39]. Thus the rate of formation of superoxide anion by complex **3** is greater The observed $E_{1/2}$ for these complexes is in the order **3** > **4** > **1** > **2** > **5**. This is in accordance with the rate of formation of $O_2^{\bullet-}$ [40]. Complex **2** shows more negative half wave potential ($E_{1/2} = -0.330$ V). This is due to the presence of electron releasing methyl group. Electron donating substituents causes a shift of $E_{1/2}$ to more negative value. Hence it is very difficult to reduce it and in turn causes less ROS generation. Complex **5** exhibits an irreversible peak with $E_{pc} = -0.192$ V showing the rate of generation of $O_2^{\bullet-}$ a minimum.

Table 2
Cyclic voltammetric data[a] for metal complexes

Complex	Peak potential (V)			
	E_{pc}	E_{pa}	ΔE_p	$E_{1/2}$
Complex **1**	−0.361	−0.170	0.191	−0.266
Complex **2**	−0.182	−0.479	0.297	−0.330
Complex **3**	−0.325	−0.091	0.234	−0.208
Complex **4**	−0.374	−0.098	0.276	−0.236
Complex **5**	−0.192	–	–	–

[a] Potentials in V against Ag/AgCl; scan rate, 100 mV/s.

3.7. Photo cleavage of DNA by metal complexes

The photo-induced DNA (pUC18, 3 μg) cleavage by complex **3** was studied in phosphate buffer (pH 7.4). The electrophoretic mobility of DNA was followed in agarose gel. The gel electrophoresis diagram for complex **3** is displayed in Fig. 9. Lanes 1 and 2 are the irradiated and dark DNA, respectively, and these lanes serve as controls. Lane 3, indicates complex **3** (1 mM) irradiated with DNA. Lanes 4 and 5 represent the concentration-dependent photocleavage by complex **3**. DNA strand scission was detected at a concentration of 3 mM. Lane 6 indicates the inhibitory effect of SOD. The intensity of lane 6 is comparable with that of control, indicating that DNA cleavage is induced by superoxide anion. The $O_2^{\bullet-}$ thus produced gives H_2O_2 ultimately yielding hydroxyl radical which is shown to be an actual DNA cleaving agent [41,42]. Addition of the hydroxyl radi-

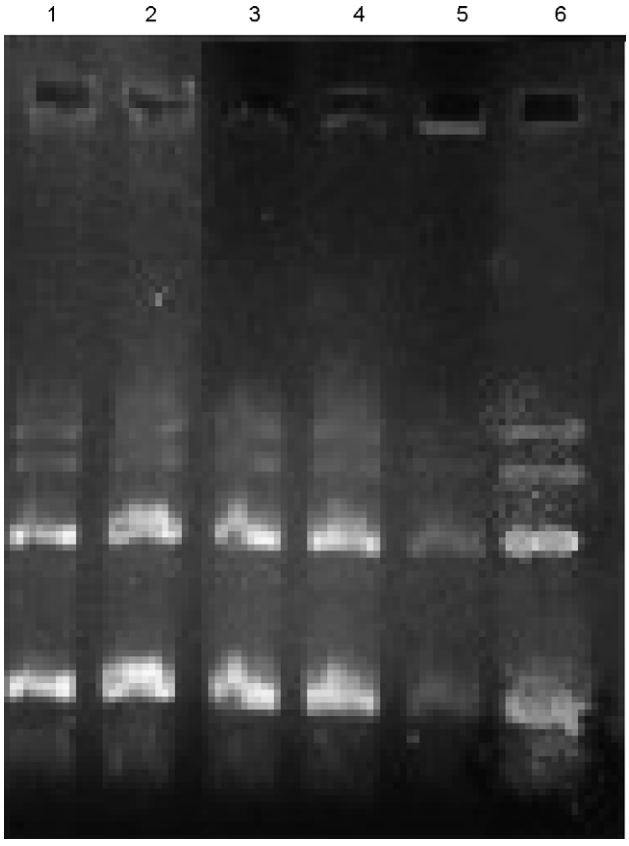

Fig. 9. Photo-induced cleavage of 3-μg plasmid DNA by complex **3** in phosphate buffer (pH 7.4) solutions. After 10 min irradiation, the loading dye was added and 20-μl aliquot of the solution was loaded into the gel. Lane 1: DNA (with irradiation); lane 2: DNA (dark); lane 3: DNA + complex 3 (1 mm) without irradiation; lane 4: DNA + complex **3** (2 mM) with irradiation; lane 5: DNA + complex **3** (3 mM) with irradiation; lane 6: DNA + complex **3** + SOD (with irradiation).

cal scavenger DMSO, however completely inhibits the cleavage reaction. On comparing the EPR–DMPO spin-trapping and cytochrome *c* reduction assay results for the formation of $O_2^{\bullet -}$, a correlation between the radical generation and DNA scission is observed. To test the possibility that photo-induced cleavage involves the formation of singlet oxygen, which is known to react with guanine residues at neutral pH, the cleavage was tested in the presence of D_2O. There was no significant enhancement of cleavage ability in D_2O, in which singlet oxygen has a significantly longer lifetime. Control experiment showed that addition of sodium azide, the known singlet oxygen quencher has no apparent inhibiting effect on photocleavage of DNA [43]. Thus the role of ROS in the *in vitro* photo-induced DNA strand scission is demonstrated. This proves that the photogenerated superoxide anion radical is inhibited by SOD, confirming that the cleavage of DNA is favoured by Type I process.

4. Conclusion

In this work we have demonstrated photosensitisation of the metal diars complexes involves both Types I and II process. RNO bleaching method, EPR spectroscopy, SOD inhibitable ferricytochrome *c* reduction assay and EPR spin-trapping experiments show that both Types I and II mechanisms are involved in the photosensitisation of metal complexes. Complexes **1** and **3** exhibit antimicrobial activity against selected bacteria *S. aureus* and *E. coli*. The superoxide anion is generated during enzymatic reduction of the complexes, correlation between antimicrobial activity of the metal complexes and enzymatic generation of ROS is observed. The complex **3** effect the cleavage of supercoiled plasmid DNA.

Acknowledgements

One of the authors (A. Suganthi) thanks UGC, New Delhi for granting the Teacher Fellowship (FIP), and Management of Thiagarajar College, Madurai, India for encouragement and permission to carry out this work. Prof. A. Bennet is gratefully acknowledged for the generous contribution of the metal complexes studied. We thank the UGC, India for the special assistance under DRS scheme to School of Chemistry, Madurai Kamaraj University.

References

[1] R.S. Nyholm, M.L. Tobe, Adv. Inorg. Chem. Radiochem. 5 (1963) 1.
[2] M. Naves, K. Libson, E. Deutsch, Nucl. Med. Biol. 14 (1987) 503–510.
[3] E. Dentsch, W. Hirth, J. Nucl. Med. 28 (1987) 1491–1500.
[4] J.R. Kircholh, W.R. Heineman, E. Dentsch, Inorg. Chem. 26 (1987) 3108–3113.
[5] B.L. Ramos, T.B. Jarbawi, W.R. Heineman, Electroanalysis 5 (1999) 320–326.
[6] B. Coyle, K. Kavanagh, M. McMann, M. Devereux, M. Geraghty, Biometals 16 (2003) 321–329.
[7] Q. Zhou, N.M. Davies, J.R. Biffin, H.L. Regtop, Chem. Res. Toxicol. 16 (2003) 28–37.
[8] P. Koczorn, W. Lewandowski, E. Lipinska, E. Sobezak, J. Agric. Food Chem. 49 (2001) 2982–2986.
[9] Q. Zhou, T.W. Hambley, B.J. Kennedy, P.L. Lay, P. Tumer, B. Warwick, J.R. Biffin, H.L. Regtop, Inorg. Chem. 39 (2000) 3742–3748.
[10] Y. Inoue, M. Hoshino, H. Takahashi, T. Noguchi, T. Murata, Y. Kanzaki, H. Hamashima, M. Sasatsu, J. Inorg. Biochem. 92 (2002) 37–42.
[11] M. Wisniewski, A. Opolski, J. Wietrzyk, J. Inorg. Biochem. 86 (2001) 480.
[12] T.C. Tsou, T.L. Yang, Chem. Biol. Interact. 102 (1998) 133–153.
[13] S. Toyokuni, J.L. Sagripanti, J. Inorg. Biochem. 47 (1992) 241–248.
[14] J.M. Mates, Toxicology 153 (2000) 83–104.
[15] P.A. Cerruti, Science 227 (1985) 375–381.
[16] J.R. Preer, H.B. Gray, J. Am. Chem. Soc. 92 (1970) 7306.
[17] B. Kalyanaraman, C.C. Felix, R.C. Sealy, Photochem. Photobiol. 36 (1982) 5–12.
[18] I. Kraljic, S. El Mohsni, Photochem. Photobiol. 28 (1978) 577–581.
[19] E. Gandin, Y. Lion, A. Van De Vorst, Photochem. Photobiol. 37 (1983) 271–278.
[20] E. Gandin, Y. Lion, J. Photochem. 30 (1982) 77–81.
[21] P.C.C. Lee, A.J. Rodgers, Photochem. Photobiol. 45 (1987) 79–86.
[22] J. Johnson Inbaraj, R. Gandhidasan, R. Murugesan, J. Photochem. Photobiol. A 124 (1999) 95–99.
[23] W.H. Koppenol, J. Butler, Isr. J. Chem. 24 (1984) 11–16.
[24] C. Murali Krishna, S. Uppuluri, P. Riesz, J.S. Zigler, D. Balasubramanian, Photochem. Photobiol. 54 (1991) 51–58.
[25] A. Constantinescu, D. Han, L. Packer, J. Biol. Chem. 268 (1993) 10906–10913.
[26] M.C. Krishna, W. DeGraff, T.S. Gonzalez, F.J. Amram Samuni, A. Russo, J.B. Mitchell, Cancer Res. 51 (1991) 6622–6628.
[27] S.M. Hahn, L. Wilson, M.C. Krishna, J. Liebnenn, W. Degraff, J. Gamson, A. Samani, D. Venzon, J.B. Mitchell, Radiat. Res. 132 (1992) 87–93.
[28] V. Schillinger, F. Lucke, Appl. Environ. Microbiol. 55 (1989) 1901–1906.
[29] T. Maniatis, E.F. Fritsch, J. Sambrook, Molecular Coloning: A Laboratory Manual, Cold Spring Harbour Laboratory, Cold Spring Harbour, NY, 1984.
[30] F. Wilkinson, J.G. Brummer, J. Phys. Chem. Ref. Data 10 (1981) 809–999.
[31] M.C. DeRosa, R.J. Crutchley, Coord. Chem. Rev. 233 (2002) 351–371.
[32] S.P. McGlynn, T. Azumi, M. Kinoshita, Molecular Spectroscopy of the Triplet State, Prentice Hall, Englewood Cliffs, 1969.
[33] R. Bonnett, A. Harriman, A.N. Kozyreu, J. Chem. Soc., Faraday Trans. 88 (1992) 763.
[34] M.B. Fleisher, K.C. Waterman, N.J. Turro, J.K. Barton, Inorg. Chem. 25 (1986) 3549–3551.
[35] Z. Diwu, J.W. Lown, Free Radic. Biol. Med. 14 (1993) 209–215.
[36] E. Ben-Hur, A. Carmichael, P. Riesz, I. Rosenthal, Int. J. Radiat. Biol. 48 (1985) 837–846.
[37] J.V. Bannister, in: R.A. Greenwald (Ed.), CRC Handbook of Methods for Oxygen Radical Research, CRC Press, Boca Raton, FL, 1985.
[38] B. Halliwell, J.M.C. Gutteridge, Free Radical in Biology and Medicine, 3rd ed., Oxford University Press, Oxford, 1999.
[39] J. Johnson Inbaraj, R. Gandhidasan, R. Murugesan, Free Radic. Biol. Med. 26 (1999) 1072–1078.
[40] G. Zagotto, S. Moro, E. Uriarte, E. Ferrazzi, G. Palu, M. Palumbo, Anticancer Drug Design 12 (1997) 99.
[41] I. Nakanishi, S. Fukuzumi, T. Konishi, K. Ohkubo, M. Fujitsuka, O. Ito, N. Miyata, J. Phys. Chem. B 106 (2002) 2372–2380.
[42] E. Gicquel, N. Paillous, P. Vicendo, Photochem. Photobiol. 72 (2000) 583–589.
[43] S. Dhar, M. Nethaji, A.R. Chakravarty, Dalton Trans. (2005) 344–348.